ACCURATE ALGORITHM FOR LOCATING FAULTS IN POWER TRANSMISSION LINES UNDER SATURATION OF CURRENT TRANSFORMERS

Jan Izykowski
Eugeniusz Rosolowski
Wroclaw University of Technology
Wroclaw, Poland
jan.izykowski@pwr.wroc.pl
eugeniusz.rosolowski@pwr.wroc.pl

Murari Mohan Saha
ABB Automation Technologies
Västerås
Sweden
murari.saha@se.abb.com

Przemyslaw Balcerek
ABB Corporate Research Center
Krakow
Poland
przemyslaw.balcerek@pl.abb.com

Abstract – This paper presents an accurate algorithm for locating faults on power transmission lines. Complete immunity to saturation of current transformers (CTs) is assured by using two-end voltages, while currents only from the terminal where the CT saturation does not happen. Such incomplete two-end signals – measured asynchronously, are processed for determining the sought distance to fault and the synchronization angle. High accuracy of the calculations is assured due to applying the distributed parameter line model. The Newton-Raphson iterative calculations are used for solving the derived equations. The delivered fault location algorithm has been tested and evaluated with the fault data obtained from versatile ATP-EMTP simulations. The sample results of the evaluation are reported and discussed.

Keywords: transmission line, fault location, two-end unsynchronised phasor measurement, ATP-EMTP, simulation

1 INTRODUCTION

Saturation of current transformers (CTs) may happen under certain fault cases of power transmission lines. The conditions, which are favourable for getting CTs saturated, are well known and recognised [1]–[4]. The CT saturation phenomenon makes some difficulties for operation of protective relays [3], as well as deteriorates accuracy of fault locators [4]–[9] – used to accurate pin-pointing of faults, what is required for the inspection-repair purpose. This paper reveals the possibility of avoiding the adverse influence of gross transformation errors of saturated CTs upon accuracy of fault locators.

Variety of fault location algorithms has been developed so far. Different availability of the measurements is considered for them, i.e. one-ended measurements [4]–[5], and much superior two-ended measurements – which are acquired synchronously [6] or asynchronously [7]–[9]. In case of one-ended measurements the specific correction of fault location errors due to CTs can be applied in order to ensure adequately high accuracy under saturation of CTs [1]–[4]. Yet another, much wider possibilities for coping with saturation of CTs appear if two-ended measurements are utilised for fault location. In [8] usage of the superimposed positive sequence voltages alone, measured asynchronously at both line terminals, has been proposed. However, uncertainty with respect to the required positive sequence impedances of the equivalent sources may be a cause of some additional errors. In order to ensure the immunity to CT saturation and simultaneously to avoid the possible drawback of the approach [8], the other method has been introduced in [9]. The algorithm from [9] has proposed to exclude currents only from the terminal with saturated CTs. It is proposed so, since in real life cases the saturation does not happen simultaneously at both ends. Thus, currents from at least one side (from the unsaturated CTs) can be used for improving the fault location accuracy.

This study presents further development of the approach introduced in [9], where the fault location algorithm has been derived with using the lumped model of the transmission line. As its innovative, this paper considers the distributed parameter line model for formulating the location algorithm. In addition, an analysis of boundary conditions of faults is carried out for determining the synchronisation angle.

The paper starts with derivation of the fault location algorithm. Then, results of extensive ATP-EMTP [10] evaluation of the algorithm are presented and discussed.

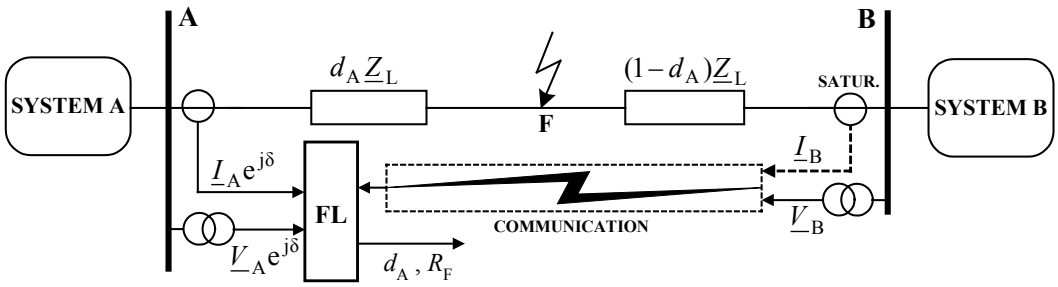

Figure 1: Schematic diagram for two-end fault location immune to saturation of CTs – the case of saturation at side B.

2 FAULT LOCATION ALGORITHM

2.1 *Generalised fault loop model*

The generalised fault loop model [9] is applied for determining the distance to fault. In further considerations the case of CT saturation at the side B (Fig.1) is taken into account. The other case (saturation of CTs at the side A) can be resolved analogously. In the considered case, the generalised model describes the fault loop seen from the terminal A:

$$\underline{V}_{\mathrm{Fp}}(d_{\mathrm{A}}) - R_{\mathrm{F}}\underline{I}_{\mathrm{F}} = 0 \qquad (1)$$

where:

$\underline{V}_{\mathrm{FAp}}(d_{\mathrm{A}})$ – voltage at the fault point F (Fig.1) for the fault loop, considered accordingly to the fault type,

d_{A} – unknown distance to fault (p.u.), as seen from A,

R_{F} – fault path resistance,

$\underline{I}_{\mathrm{F}}$ – fault path current (total fault current).

The voltage at the fault point F (Fig.1), for the considered fault loop, can be composed as follows [9]:

$$\underline{V}_{\mathrm{Fp}}(d_{\mathrm{A}}) = \underline{\mathrm{a}}_1\underline{V}_{\mathrm{F1}} + \underline{\mathrm{a}}_2\underline{V}_{\mathrm{F2}} + \underline{\mathrm{a}}_0\underline{V}_{\mathrm{F0}} \qquad (2)$$

where:

$\underline{\mathrm{a}}_1$, $\underline{\mathrm{a}}_2$, $\underline{\mathrm{a}}_0$ – weighting coefficients dependent on fault type (gathered in Table 1).

Applying the distributed parameter model of a line the symmetrical components of voltages from (2) are:

$$\underline{V}_{\mathrm{F1}} = (\underline{V}_{\mathrm{A1}}\cosh(\gamma_1\ell d_{\mathrm{A}}) - \underline{Z}_{\mathrm{c1}}\underline{I}_{\mathrm{A1}}\sinh(\gamma_1\ell d_{\mathrm{A}}))\mathrm{e}^{\mathrm{j}\delta} \qquad (3)$$

$$\underline{V}_{\mathrm{F2}} = (\underline{V}_{\mathrm{A2}}\cosh(\gamma_1\ell d_{\mathrm{A}}) - \underline{Z}_{\mathrm{c1}}\underline{I}_{\mathrm{A2}}\sinh(\gamma_1\ell d_{\mathrm{A}}))\mathrm{e}^{\mathrm{j}\delta} \qquad (4)$$

$$\underline{V}_{\mathrm{F0}} = (\underline{V}_{\mathrm{A0}}\cosh(\gamma_0\ell d_{\mathrm{A}}) - \underline{Z}_{\mathrm{c0}}\underline{I}_{\mathrm{A0}}\sinh(\gamma_0\ell d_{\mathrm{A}}))\mathrm{e}^{\mathrm{j}\delta} \qquad (5)$$

where:

$\mathrm{e}^{\mathrm{j}\delta}$ – synchronisation operator providing that the measurements of the side A have the common time reference with the side B (assumed here as the basis),

$\underline{V}_{\mathrm{A1}}$, $\underline{V}_{\mathrm{A2}}$, $\underline{V}_{\mathrm{A0}}$ – symmetrical components of side A voltages (subscripts denoting the component type: 1–positive, 2–negative, 0–zero sequence),

$\underline{I}_{\mathrm{A1}}$, $\underline{I}_{\mathrm{A2}}$, $\underline{I}_{\mathrm{A0}}$ – symmetrical components of side A currents,

$\underline{Z}_{c1} = \sqrt{\underline{Z}'_{1\mathrm{L}}/\underline{Y}'_{1\mathrm{L}}}$ – surge impedance of the line for the positive (negative) sequences,

$\underline{Z}_{c0} = \sqrt{\underline{Z}'_{0\mathrm{L}}/\underline{Y}'_{0\mathrm{L}}}$ – surge impedance of the line for the zero sequence,

$\gamma_1 = \sqrt{\underline{Z}'_{1\mathrm{L}}\underline{Y}'_{1\mathrm{L}}}$ – propagation constant of the line for the positive (negative) sequence,

$\gamma_0 = \sqrt{\underline{Z}'_{0\mathrm{L}}\underline{Y}'_{0\mathrm{L}}}$ – propagation constant of the line for the zero sequence,

$\underline{Z}'_{1\mathrm{L}}$, $\underline{Z}'_{0\mathrm{L}}$ – impedance data (for the positive (negative) and zero sequences) of the line per km length,

$\underline{Y}'_{1\mathrm{L}}$, $\underline{Y}'_{0\mathrm{L}}$ – admittance data (for the positive (negative) and zero sequences) of the line per km length,

ℓ – total line length (km).

Note: in the above considerations, as well as in all further ones, it is assumed that the parameters of the line for the negative sequence are identical with the positive sequence data. For the transmission lines this is the case, and thus there is no need to use different subscripts for the positive and negative sequence data.

In order to determine the unknown distance to fault (d_{A}) from the generalised fault loop model (1), the synchronisation operator ($\exp(\mathrm{j}\delta)$) and the total fault current ($\underline{I}_{\mathrm{F}}$) have to be determined.

FAULT	$\underline{a}_1$	$\underline{a}_2$	$\underline{a}_0$
a-g	1	1	1
b-g	$\underline{\mathrm{a}}^2$	$\underline{\mathrm{a}}$	1
c-g	$\underline{\mathrm{a}}$	$\underline{\mathrm{a}}^2$	1
a-b, a-b-g a-b-c, a-b-c-g	$1-\underline{\mathrm{a}}^2$	$1-\underline{\mathrm{a}}$	0
b-c, b-c-g	$\underline{\mathrm{a}}^2-\underline{\mathrm{a}}$	$\underline{\mathrm{a}}-\underline{\mathrm{a}}^2$	0
c-a, c-a-g	$\underline{\mathrm{a}}-1$	$\underline{\mathrm{a}}^2-1$	0
$\underline{\mathrm{a}} = \exp(\mathrm{j}2\pi/3)$; $\mathrm{j} = \sqrt{-1}$			

Table 1: Weighting coefficients for composing signal (2).

2.2 *Determination of the synchronisation operator and the total fault current*

It is proposed to determine the unknown synchronisation operator by exploring the boundary conditions of faults. For this purpose the symmetrical components (in general: the *i*-th type) of the total fault current have to be determined. According to the distributed parameter model of the faulted line (Fig.2) one obtains:

$$\underline{V}_{\mathrm{Fi}} = (\underline{V}_{\mathrm{Ai}}\cosh(\gamma_i\ell d_{\mathrm{A}}) - \underline{Z}_{\mathrm{ci}}\underline{I}_{\mathrm{Ai}}\sinh(\gamma_i\ell d_{\mathrm{A}}))\mathrm{e}^{\mathrm{j}\delta} \qquad (6)$$

$$\underline{I}_{\mathrm{AFi}} = (-(1/\underline{Z}_{\mathrm{ci}})\underline{V}_{\mathrm{Ai}}\sinh(\gamma_i\ell d_{\mathrm{A}}) + \underline{I}_{\mathrm{Ai}}\cosh(\gamma_i\ell d_{\mathrm{A}}))\mathrm{e}^{\mathrm{j}\delta} \qquad (7)$$

Taking (6) and (7), the voltage at the remote terminal B can be determined as follows:

$$\begin{aligned}\underline{V}_{\mathrm{Bi}} &= \underline{V}_{\mathrm{Fi}}\cosh(\gamma_i\ell(1-d_{\mathrm{A}})) \\ &\quad - \underline{Z}_{\mathrm{ci}}(\underline{I}_{\mathrm{AFi}} - \underline{I}_{\mathrm{Fi}})\sinh(\gamma_i\ell(1-d_{\mathrm{A}}))\end{aligned} \qquad (8)$$

From (8) the *i*-th symmetrical component of the total fault current is determined as:

$$\underline{I}_{\mathrm{Fi}} = \frac{\underline{V}_{\mathrm{Bi}} + \underline{N}_{\mathrm{Ai}}\mathrm{e}^{\mathrm{j}\delta}}{\underline{Z}_{\mathrm{ci}}\sinh(\gamma_i\ell(1-d_{\mathrm{A}}))} \qquad (9)$$

where:

$$\underline{N}_{\mathrm{Ai}} = -\underline{V}_{\mathrm{Ai}}\cosh(\gamma_i\ell) + \underline{Z}_{\mathrm{ci}}\underline{I}_{\mathrm{Ai}}\sinh(\gamma_i\ell) \qquad (9a)$$

In general, the total fault current is a composition of its respective components:

$$\underline{I}_{\mathrm{F}} = \underline{a}_{\mathrm{F1}}\underline{I}_{\mathrm{F1}} + \underline{a}_{\mathrm{F2}}\underline{I}_{\mathrm{F2}} + \underline{a}_{\mathrm{F0}}\underline{I}_{\mathrm{F0}} \qquad (10)$$

where:

$\underline{a}_{\mathrm{F1}}$, $\underline{a}_{\mathrm{F2}}$, $\underline{a}_{\mathrm{F0}}$ – share coefficients dependent on fault.

There is certain freedom in selecting the share coefficients and it is advantageous to exclude the zero sequence [5], [9]; i.e. to choose: $\underline{a}_{\mathrm{F0}} = 0$.

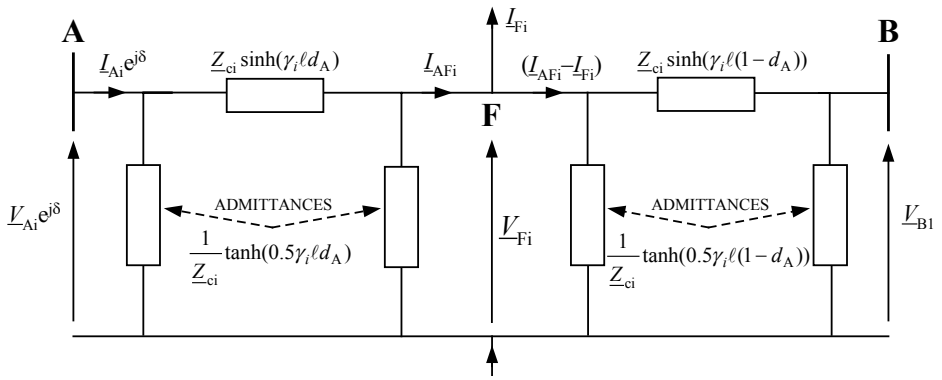

Figure 2: Equivalent circuit diagram of transmission line for the *i*-th symmetrical component.

Therefore, in all further considerations exclusion of the zero sequence components [5], [9] is applied. Thus:

$$\underline{I}_{\mathrm{F}} = \underline{a}_{\mathrm{F1}}\underline{I}_{\mathrm{F1}} + \underline{a}_{\mathrm{F2}}\underline{I}_{\mathrm{F2}} \tag{11}$$

There two characteristic sets (among the other possible) of the share coefficients for the phase-to-ground and phase-to-phase faults, as gathered in Table 2.

FAULT	I–SET		II–SET	
	$\underline{a}_{\mathrm{F1}}^{\mathrm{I-SET}}$	$\underline{a}_{\mathrm{F2}}^{\mathrm{I-SET}}$	$\underline{a}_{\mathrm{F1}}^{\mathrm{II-SET}}$	$\underline{a}_{\mathrm{F2}}^{\mathrm{II-SET}}$
a–g	0	3	3	0
b–g	0	$3\underline{a}$	$3\underline{a}^2$	0
c–g	0	$3\underline{a}^2$	$3\underline{a}$	0
a–b	0	$1-\underline{a}$	$1-\underline{a}^2$	0
b–c	0	$\underline{a}-\underline{a}^2$	$\underline{a}^2-\underline{a}$	0
c-a	0	$\underline{a}^2-1$	$\underline{a}-1$	0

Table 2: Two sets of share coefficients for phase-to-ground faults and phase-to-phase faults.

Applying the sets from Table 2 the total fault current can be expressed as follows:

$$\underline{I}_{\mathrm{F}} = \underline{a}_{\mathrm{F1}}^{\mathrm{I-SET}}\underline{I}_{\mathrm{F1}} + \underline{a}_{\mathrm{F2}}^{\mathrm{I-SET}}\underline{I}_{\mathrm{F2}} \tag{12}$$

or alternatively:

$$\underline{I}_{\mathrm{F}} = \underline{a}_{\mathrm{F1}}^{\mathrm{II-SET}}\underline{I}_{\mathrm{F1}} + \underline{a}_{\mathrm{F2}}^{\mathrm{II-SET}}\underline{I}_{\mathrm{F2}} \tag{13}$$

Example: a-g fault

Using the I–SET of the share coefficients one gets:

$$\underline{I}_{\mathrm{F}} = \underline{a}_{\mathrm{F1}}^{\mathrm{I-SET}}\underline{I}_{\mathrm{F1}} + \underline{a}_{\mathrm{F2}}^{\mathrm{I-SET}}\underline{I}_{\mathrm{F2}} = 3\underline{I}_{\mathrm{F2}} \tag{14}$$

while using the II–SET:

$$\underline{I}_{\mathrm{F}} = \underline{a}_{\mathrm{F1}}^{\mathrm{II-SET}}\underline{I}_{\mathrm{F1}} + \underline{a}_{\mathrm{F2}}^{\mathrm{II-SET}}\underline{I}_{\mathrm{F2}} = 3\underline{I}_{\mathrm{F1}} \tag{15}$$

This means that for the considered a-g fault we get:

$$\underline{I}_{\mathrm{F1}} = \underline{I}_{\mathrm{F2}} \tag{16}$$

Taking (9) for: i=1 (positive sequence), i=2 (negative sequence) and substituting into (16) one obtains:

$$\frac{\underline{V}_{\mathrm{B1}} + \underline{N}_{\mathrm{A1}}[\mathrm{e}^{\mathrm{j}\delta}]_{\mathrm{a-g}}}{\underline{Z}_{\mathrm{c1}}\sinh(\gamma_1\ell(1-d_{\mathrm{A}}))} = \frac{\underline{V}_{\mathrm{B2}} + \underline{N}_{\mathrm{A2}}[\mathrm{e}^{\mathrm{j}\delta}]_{\mathrm{a-g}}}{\underline{Z}_{\mathrm{c1}}\sinh(\gamma_1\ell(1-d_{\mathrm{A}}))} \tag{17}$$

From (17) one obtains the synchronisation operator:

$$[\mathrm{e}^{\mathrm{j}\delta}]_{\mathrm{a-g}} = \frac{\underline{V}_{\mathrm{B2}} - \underline{V}_{\mathrm{B1}}}{\underline{N}_{\mathrm{A1}} - \underline{N}_{\mathrm{A2}}} \tag{18}$$

where:

$$\underline{N}_{\mathrm{A1}} = -\underline{V}_{\mathrm{A1}}\cosh(\gamma_1\ell) + \underline{Z}_{\mathrm{c1}}\underline{I}_{\mathrm{A1}}\sinh(\gamma_1\ell) \tag{18a}$$

$$\underline{N}_{\mathrm{A2}} = -\underline{V}_{\mathrm{A2}}\cosh(\gamma_1\ell) + \underline{Z}_{\mathrm{c1}}\underline{I}_{\mathrm{A2}}\sinh(\gamma_1\ell) \tag{18b}$$

In general terms, for all faults considered in Table 2, one gets the following formula for the synchronisation operator:

$$[\mathrm{e}^{\mathrm{j}\delta}]_{\mathrm{ph-g,\,ph-ph}} = \frac{\underline{a}_{\mathrm{F2}}^{\mathrm{I-SET}}\underline{V}_{\mathrm{B2}} - \underline{a}_{\mathrm{F1}}^{\mathrm{II-SET}}\underline{V}_{\mathrm{B1}}}{\underline{a}_{\mathrm{F1}}^{\mathrm{II-SET}}\underline{N}_{\mathrm{A1}} - \underline{a}_{\mathrm{F2}}^{\mathrm{I-SET}}\underline{N}_{\mathrm{A2}}} \tag{19}$$

Determination of the synchronisation operator for such faults, according to (19), requires using the coefficients from Table 2 and the formula (18a), (18b).

In contrast to the above fault types, the other situation is for the remaining fault types (phase-to-phase-to-ground and three phase symmetrical faults). This is so, since for these remaining faults there is no alternative sets of the share coefficients for the positive and the negative sequence – see Table 3.

FAULT	$\underline{a}_{\mathrm{F1}}$	$\underline{a}_{\mathrm{F2}}$
a–b–g, a–b–c, a–b–c–g	$1-\underline{a}^2$	$1-\underline{a}$
b–c-g	$\underline{a}^2-\underline{a}$	$\underline{a}-\underline{a}^2$
c-a-g	$\underline{a}-1$	$\underline{a}^2-1$

Table 3: Set of share coefficients for phase-to-phase-to-ground faults and three phase faults.

In case of phase-to-phase-to-ground faults an analysis of the boundary conditions yields the following relation between the symmetrical components of the total fault current:

$$\underline{I}_{\mathrm{F0}} = \underline{b}_{\mathrm{F1}}\underline{I}_{\mathrm{F1}} + \underline{b}_{\mathrm{F2}}\underline{I}_{\mathrm{F2}} \tag{20}$$

where:

$\underline{b}_{\mathrm{F1}}$, $\underline{b}_{\mathrm{F2}}$ – coefficients delivered in Table 4.

FAULT	$\underline{b}_{\mathrm{F1}}$	$\underline{b}_{\mathrm{F2}}$
a–b–g	$-\underline{a}$	$-\underline{a}^2$
b–c–g	–1	–1
c–a–g	$-\underline{a}^2$	$-\underline{a}$

Table 4: Coefficients for determining the relation between the symmetrical components of the total fault current (20).

Substituting (9) into (20) results in:

$$\frac{\underline{V}_{B0}+\underline{N}_{A0}[e^{j\delta}]_{ph-ph-g}}{\underline{Z}_{c0}\sinh(\gamma_0\ell(1-d_A))}= \tag{21}$$

$$=\frac{\underline{b}_{F1}\underline{V}_{B1}+\underline{b}_{F2}\underline{V}_{B2}+(\underline{b}_{F1}\underline{N}_{A1}+\underline{b}_{F2}\underline{N}_{A2})[e^{j\delta}]_{ph-ph-g}}{\underline{Z}_{c1}\sinh(\gamma_1\ell(1-d_A))}$$

Direct determination of the synchronisation operator from (21), i.e. without knowing the distance to fault (d_A), can not be accomplished.

In case of three-phase balanced faults, the positive sequence components are the only ones present in the measured currents and voltages. From these reason, it is impossible to apply the methodology explored for the already considered fault types. The only possibility is to write down the equations of the line for the pre-fault state, as for example for the positive sequence:

$$\begin{aligned}\underline{V}_{B1_pre}&=\underline{V}_{A1_pre}\cosh(\gamma_1\ell)[e^{j\delta}]_{3ph}\\&\quad-\underline{Z}_{c1}\underline{I}_{A1_pre}\sinh(\gamma_1\ell)[e^{j\delta}]_{3ph}\end{aligned} \tag{22}$$

$$[e^{j\delta}]_{3ph}=\frac{\underline{V}_{B1_pre}}{\underline{V}_{A1_pre}\cosh(\gamma_1\ell)-\underline{Z}_{c1}\underline{I}_{A1_pre}\sinh(\gamma_1\ell)} \tag{23}$$

2.3 Estimation of the total fault current

Having the synchronisation operator determined, then the total fault current could be estimated. Substituting (9) into (11) results in the following formula:

$$\underline{I}_F=\frac{\underline{a}_{F1}(\underline{V}_{B1}+\underline{N}_{A1}e^{j\delta})+\underline{a}_{F2}(\underline{V}_{B2}+\underline{N}_{A2}e^{j\delta})}{\underline{Z}_{c1}\sinh(\gamma_1\ell(1-d_A))} \tag{24}$$

which for the sake of its shortening is rewritten as:

$$\underline{I}_F=\frac{\underline{M}_{12}(e^{j\delta})}{\underline{Z}_{c1}\sinh(\gamma_1\ell(1-d_A))} \tag{24a}$$

where:

$$\underline{M}_{12}(e^{j\delta})=\underline{a}_{F1}(\underline{V}_{B1}+\underline{N}_{A1}e^{j\delta})+\underline{a}_{F2}(\underline{V}_{B2}+\underline{N}_{A2}e^{j\delta})$$

$\underline{N}_{A1}$, $\underline{N}_{A2}$ – defined in (18a), (18b),

$\underline{a}_{F1}$, $\underline{a}_{F2}$ – share coefficients dependent on fault type (taken from Table 2 (any set) or from Table 3).

2.4 Determination of the distance to fault

Substituting the total fault current (24a) into the general fault loop model (1) one gets:

$$\underline{V}_{Fp}(d_A,e^{j\delta})-R_F\frac{\underline{M}_{12}(e^{j\delta})}{\underline{Z}_{c1}\sinh(\gamma_1\ell(1-d_A))}=0 \tag{25}$$

After rearranging one gets:

$$\underline{Z}_{c1}\sinh(\gamma_1\ell(1-d_A))\underline{V}_{Fp}(d_A,e^{j\delta})-R_F\underline{M}_{12}(e^{j\delta})=0 \tag{26}$$

$\underline{V}_{FAp}(d_A,e^{j\delta})$ – defined in (2)–(5).

There are two characteristic cases:

I) all faults except phase-to-phase-to-ground faults,

II) phase-to-phase-to-ground faults.

In the first case (I) the synchronisation angle is determined without involving the unknown distance to fault. Therefore, the formula (26) contains two unknowns: d_A – distance to fault, R_F – fault resistance, and can be written down in the general form:

$$\underline{F}_I(d_A,R_F)=\underline{F}_{I_real}(d_A,R_F)+j\underline{F}_{I_imag}(d_A,R_F)=0 \tag{27}$$

Applying the well known Newton-Raphson method, the iterative calculations for solving (27) are performed according to the following matrix formula:

$$\mathbf{X}_{I_new}=\mathbf{X}_{I_old}-\mathbf{J}^{-1}(\mathbf{F}_{I_old})*\mathbf{F}_{I_old} \tag{28}$$

where:

$$\mathbf{X}_{I_new}=\begin{bmatrix}d_{A_new}\\R_{F_new}\end{bmatrix},\qquad \mathbf{X}_{I_old}=\begin{bmatrix}d_{A_old}\\R_{F_old}\end{bmatrix},$$

$$\mathbf{F}_{I_old}=\begin{bmatrix}F_{I_real}(d_{A_old},R_{F_old})\\F_{I_imag}(d_{A_old},R_{F_old})\end{bmatrix},$$

$$\mathbf{J}(\mathbf{F}_{I_old})=\begin{bmatrix}\dfrac{\partial F_{I_real}(d_{A_old},R_{F_old})}{\partial d_{A_old}} & \dfrac{\partial F_{I_real}(d_{A_old},R_{F_old})}{\partial R_{F_old}}\\[2ex] \dfrac{\partial F_{I_imag}(d_{old},R_{F_old})}{\partial d_{A_old}} & \dfrac{\partial F_{I_imag}(d_{A_old},R_{F_old})}{\partial R_{F_old}}\end{bmatrix}.$$

As the starting values for the unknown fault distance and resistance one can apply the ones obtained from solution of the linearised form of (27), which can be obtained after substitutions:

$$\sinh(\gamma_1\ell d_A)\to(\gamma_1\ell d_A)$$
$$\sinh(\gamma_1\ell(1-d_A))\to(\gamma_1\ell(1-d_A))$$
$$\cosh(\gamma_1\ell d_A)\to 1$$

In the second case (II), the synchronisation angle can not be determined directly, i.e. without involving the unknown distance to fault. Therefore, the formula (27) contains four unknowns: d_A – distance to fault, R_F – fault resistance, $\cos(\delta)$ and $\sin(\delta)$. It can be written down in the general form as follows:

$$\begin{aligned}&\underline{F}_{II}(d_A,R_F,\cos(\delta),\sin(\delta))=\\&=\underline{F}_{II_real}(d_A,R_F,\cos(\delta),\sin(\delta))\\&\quad+j\underline{F}_{II_imag}(d_A,R_F,\cos(\delta),\sin(\delta))=0\end{aligned} \tag{29}$$

In order to manage solution for the four unknowns, present in this case, additionally the relation (21) has to be utilised:

$$\begin{aligned}&\underline{F}_{II_a}(d_A,R_F,\cos(\delta),\sin(\delta))=\frac{\underline{V}_{B0}+\underline{N}_{A0}(e^{j\delta})}{\underline{Z}_{c0}\sinh(\gamma_0\ell(1-d_A))}\\&-\frac{\underline{b}_{F1}(\underline{V}_{B1}+\underline{N}_{A1}e^{j\delta})+\underline{b}_{F2}(\underline{V}_{B2}+\underline{N}_{A2}e^{j\delta})}{\underline{Z}_{c1}\sinh(\gamma_1\ell(1-d_A))}=0\end{aligned} \tag{30}$$

The iterative calculations can be performed analogously as in the first case (I). Again, the linearisation of (29) and (30) has to be accomplished for obtaining the initial values of the unknowns, which are then used for starting the iterative calculations.

3 ATP-EMTP EVALUATION

The presented fault location algorithm has been evaluated with using the fault data obtained from ATP-EMTP [10] versatile simulations of faults in the power network containing the 400 kV, 300 km transmission line. The parameters of the network are gathered in Table 5. Capacitive voltage transformers (CVTs) and non-linear CTs have been modelled together with the

second order analogue anti-aliasing filters with the cut-off frequency set to 350 Hz. Signals were sampled at 1000 Hz and the full-cycle Fourier orthogonal filters with dc rejection were applied for determining phasors.

Different specifications of faults have been considered in the study. Selected results are depicted in Fig.3–Fig.7. Fig.3 shows the fault location accuracy with use of the delivered algorithm. In one case there is the CT saturation at the side A (at d_A=0.1 p.u.) and due to that considering the fault loop seen from this side results in the error of around 2.5%. However, for the fault loop seen from the side B (the currents from the saturated CTs of the side A are rejected) the error drops below 0.5%, if the distributed parameter line model is utilized.

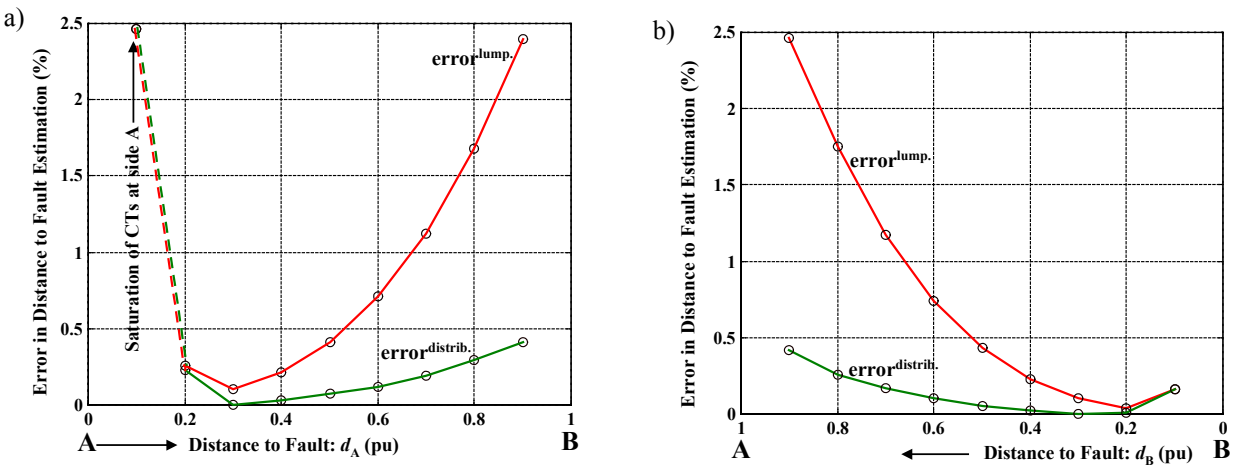

Figure 3: Error in distance to fault estimation with considering the fault loop seen from: a) terminal A, b) terminal B. Fault: a–b, R_F=0.5 Ω, distance to fault: 0.1 ÷ 0.9 (p.u.). Values of the error under considering the lumped (lump.) and distibuted (distrib.) parameter models of the line.

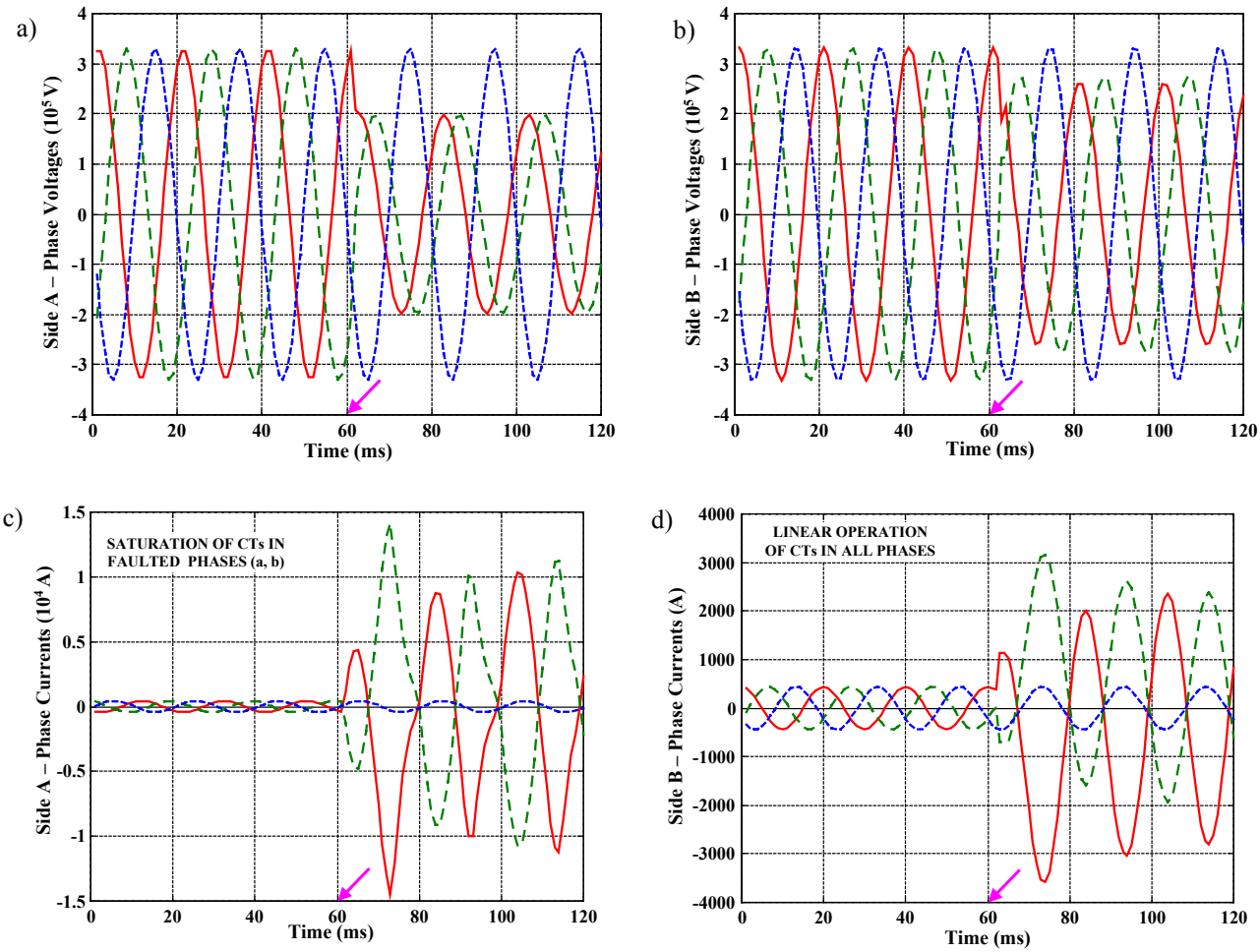

Figure 4: Example of fault location with CTs saturation: a) side A voltages, b) side B voltages, c) side A currents, d) side B currents. Fault: a–b, R_F=0.5 Ω, d_A=0.1 (p.u.).

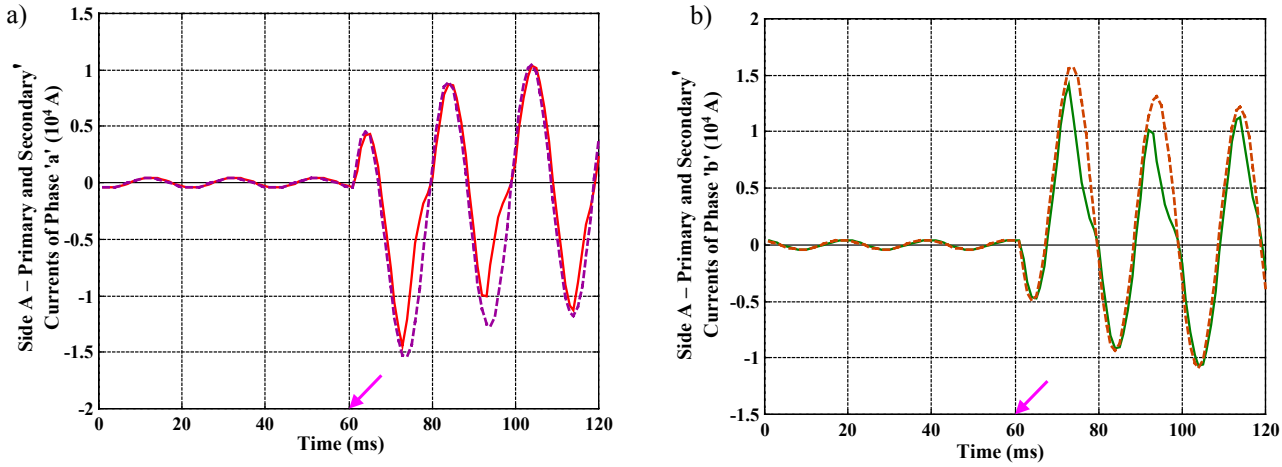

Figure 5: Example of fault location with CTs saturation – waveforms of primary and secondary' (recalculated to the primary level) from the faulted phases: a) phase 'a', b) phase 'b'.

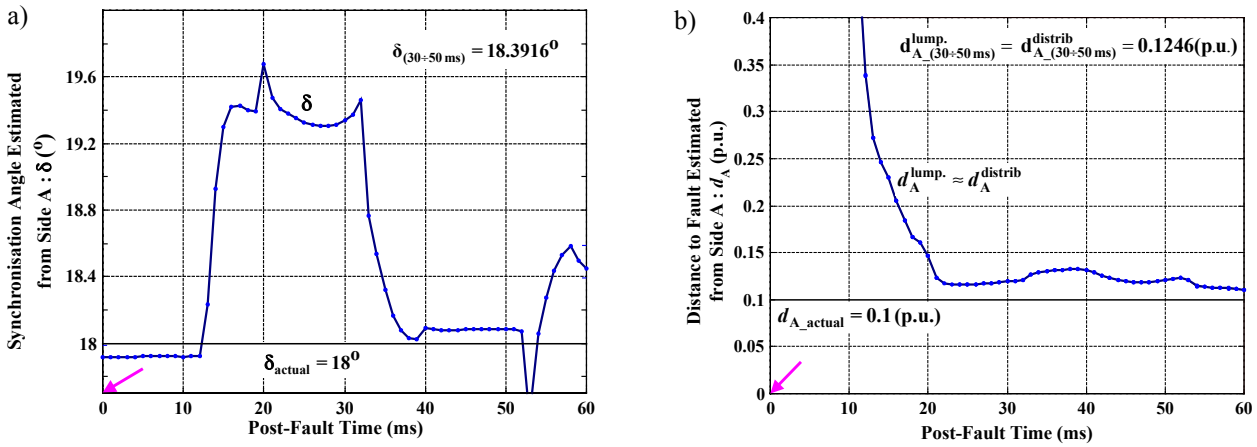

Figure 6: Example of fault location with CTs saturation (at the side A) – fault location from the side A: a) synchronisation angle, b) estimated distance to fault for the lumped and distributed parameter line models.

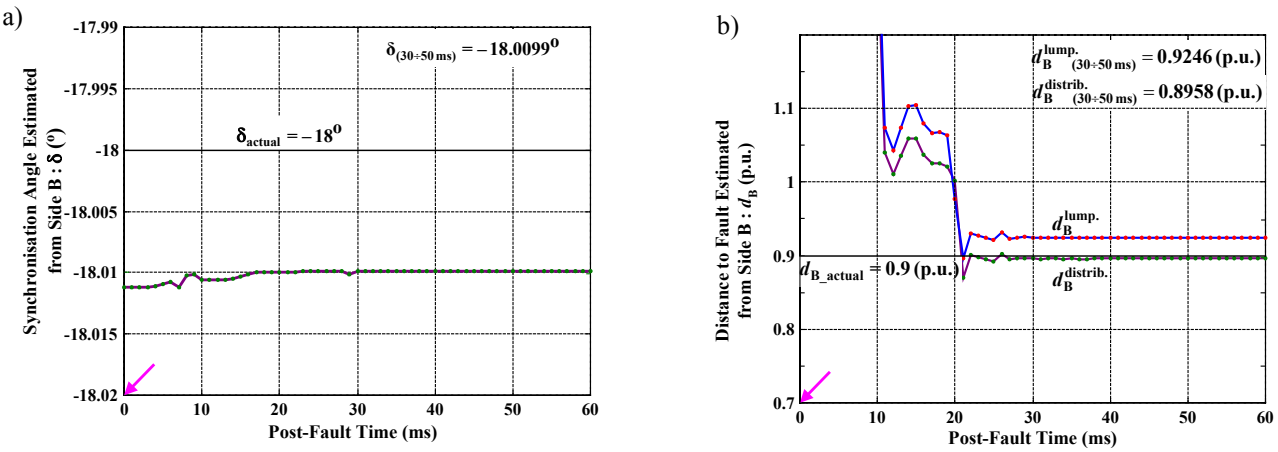

Figure 7: Example of fault location with CTs saturation (at the side A) – fault location from the side B: a) synchronisation angle, b) estimated distance to fault for the lumped and distributed parameter line models.

For the other fault cases the saturation does not happen and the errors reach the level of 2.5% – under considering the lumped line model but do not exceed 0.5% – under taking into account the distributed parameter line model.

The signals obtained from ATP-EMTP simulations are in natural way perfectly synchronized. In order to show performance of the presented algorithm, the voltage and current signals measured at the terminal A were artificially delayed by 18° (note: this delay corresponds to the single sampling interval for 50 Hz signals digitalized at 1000 Hz). The single value results were obtained by averaging within the interval (30 ÷ 50) ms after the fault inception.

It has been verified, that it is sufficient to perform only a single iteration of the Newton-Raphson calculations of the distance to fault.

Component	Parameter	
Line AB	ℓ	300 km
	$\underline{Z}'_{1L}$	(0.0276+j0.3151) Ω/km
	$\underline{Z}'_{0L}$	(0.2750+j1.0265) Ω/km
	C'_{1L}	13.0 nF/km
	C'_{0L}	8.5 nF/km
Equivalent system at terminal A	$\underline{Z}_{1SA}$	(2.6047+j14.772) Ω
	$\underline{Z}_{0SA}$	(4.6364+j26.2944) Ω
	Angle of EMFs	0°
Equivalent system at terminal B	$\underline{Z}_{1SB}$	2 $\underline{Z}_{1SA}$
	$\underline{Z}_{0SB}$	2 $\underline{Z}_{0SA}$
	Angle of EMFs	-30°

Table 5: Parameters of the transmission network.

4 CONCLUSIONS

In the paper the new accurate algorithm for locating faults on power transmission line, with use of unsynchronized measurements of two-end voltages and currents from the terminal with no CT saturation, has been presented. Usage of such incomplete two-end measurements assures immunity to CT saturation, which in real life situations could happen on one side of the line only.

Innovative contribution of this paper relies on the followings:

- determination of the synchronization angle from analysis of the boundary conditions of faults, performed with considering the distributed parameter line model,
- determination of the distance to fault with also strict consideration of distributed nature of the transmission line.

The Newton-Raphson iterative calculations have been applied for solving the derived non-linear equations. The initial values for the sought quantities are obtained by considering the linearised forms of these equations. Very fast convergence of the iterative calculations has been observed. In practice, it is sufficient to perform only a single iteration, what in fact leads to the algorithm of non-iterative feature.

Two-terminal line case has been considered, however, the presented method can be easily extended for application to double-circuit, as well as multi-terminal lines. This can be considered as the future investigations of the delivered fault location technique.

The performed testing and evaluation with the fault data obtained from ATP-EMTP simulations proved satisfactory performance and high accuracy of the presented fault location algorithm. Due to taking into account the distributed parameter line model the errors in distance to fault estimation for the 300 km transmission line do not exceed 0.5%.

ACKNOWLEDGMENT

This work was supported in part by the Ministry of Science and Information Society Technologies of Poland under Grant 3 T10B 030 27.

REFERENCES

[1] Y.C. Kang, S.H. Kang, J.K. Park, A.T. Jones and R.K. Aggarwal, "Development and hardware implementation of a compensating algorithm for the secondary current of current transformers", IEE Proc. – Electric Power Applications, Vol. 143, No.1, pp. 41–49, 1996

[2] B. Kasztenny, E. Rosolowski, M. Lukowicz and J. Izykowski, "Current related relaying algorithms immune to saturation of current transformers", IEE Conference Publication No. 434, pp. 365–369, 1997

[3] T. Bunyagul and P.A. Crossley, "Design and evaluation of an overcurrent relay suitable for operation with measurement current transformers", IEE Conference Publication No. 479, pp. 201–204, 2001

[4] A. Wiszniewski, "Fault location correction of errors due to current transformers", Developments in Power System Protection Preceedings, Conference Publ. No. 249, pp. 185–187, 1985

[5] L. Eriksson, M.M. Saha and G.D. Rockefeller, "An accurate fault locator with compensation for apparent reactance in the fault resistance resulting from remote-end infeed", IEEE Trans. on PAS, vol. PAS-104, pp. 424-436, No. 2, 1985

[6] M. Kezunovic and B. Perunicic, "Automated transmission line fault analysis using synchronized sampling at two ends", IEEE Trans. on Power Systems, pp. 441–447, PS–11, 1996

[7] D. Novosel, D.G. Hart, E. Udren and J. Garitty J, "Unsynchronized two-terminal fault location estimation", IEEE Trans. on Power Delivery, vol. 11, pp. 130–138, No. 1, 1996

[8] I. Zamora, J.F. Minambres, A.J. Mazon, R. Alvarez-Isasi and J. Lazaro, "Fault location on two-terminal transmission lines based on voltages", IEE Proc. Gener. Transm. Distrib., vol. 143, pp. 1–6, No. 1, 1996

[9] M.M. Saha, J. Izykowski and E. Rosolowski, "A two-end method of fault location immune to saturation of current transformers", Developments in Power System Protection Proceedings, Amsterdam, pp. 172–175, 2004

[10] H. Dommel, "Electro-Magnetic Transients Program", BPA, Portland, Oregon, 1986.